JOURNAL OF PROPULSION AND POWER
Vol. 9, No. 5, Sept.–Oct. 1993

# Application of a Quadruple Probe Technique to MPD Thruster Plume Measurements

Rodney L. Burton* and Susan G. DelMedico†
*University of Illinois at Urbana—Champaign, Urbana, Illinois 61801*
and
J. Chris Andrews‡
*Phillips Laboratory, Edwards Air Force Base, California 93524*

**A new quadruple Langmuir probe diagnostic technique is applied to the plume of a pulsed magnetoplasmadynamic (MPD) thruster with argon propellant. The probe permits simultaneous measurement of electron temperature $T_e$, density $n_e$, and ion flow velocity $u$ in the exhaust stream. For distances of 3–25 cm from the thruster face, $T_e$ is 8–1.5 eV, $n_e$ is $4.8–1.2 \times 10^{19}$ m$^{-3}$, and $u$ is $0.7–1.8 \times 10^4$ m/s. The measurements suggest that the plume is well-collimated, and that the ion temperature is significantly higher than the electron temperature, consistent with an ion-conduction model of the thruster.**

## Nomenclature

$A$ = probe surface area, m$^2$
$A_\parallel$, $A_\perp$ = collection area of parallel, perpendicular probes, m$^2$
$B$, $B_\theta$, $\mathbf{B}$ = azimuthal magnetic field, T
$C_p$ = argon translational specific heat, 5°R/2
$c_m$ = most probable argon thermal speed $\sqrt{2kT/m}$, m/s
$e$ = electronic charge, $1.602 \times 10^{-19}$ C
$h$ = enthalpy, J/kg
$I$ = thruster current, A
$I_{1,3,4}$ = current to probes 1, 3, and 4, A
$I_\perp$ = current to probe oriented perpendicularly to flow, A
$I_\parallel$ = current to probe oriented parallel to flow, A
$j$, $\mathbf{j}$ = total current density, A/m$^2$
$j_e$ = electron saturation current density, A/m$^2$
$j_i$ = ion saturation current density, A/m$^2$
$k$ = Boltzmann's constant, $1.38 \times 10^{-23}$ J/K
$L$ = probe length, m
$\dot{m}$ = argon mass flow rate, kg/s
$m_i$ = argon ion mass, $6.6 \times 10^{-26}$ kg
$n$ = total heavy particle density, m$^{-3}$; summation integer
$n_e$ = electron density, m$^{-3}$
$n_i$ = ion density, m$^{-3}$
$r$, $x$ = radial, axial plume coordinates, cm
$r_p$ = probe radius, m
$T$, $T_0$ = heavy particle temperature, total temperature, eV
$T_e$, $T_i$ = electron, ion temperature, eV
$u$ = axial plasma flow velocity, m/s
$V$ = voltage
$V_{d2}$ = potential difference between probes 1 and 2, V
$V_{d3}$ = fixed potential difference between probes 1 and 3, V
$V_{d4}$ = fixed potential difference between probes 1 and 4, V
$x_0$ = location of virtual center of plume expansion, cm
$\alpha$, $\alpha^{++}$ = first, second degree of ionization
$\gamma$ = ratio of specific heats
$\varepsilon_0$ = permittivity constant, $8.85 \times 10^{-12}$ F/m
$\eta$ = frozen flow efficiency
$\theta$ = angle of probe to flow velocity
$\kappa$ = velocity ratio, $u/c_m \sin\theta$
$\lambda_D$ = Debye length, m
$\lambda_{ee}$ = electron-electron mean free path, m
$\lambda_{ii}$ = ion-ion mean free path, m
$\mu_0$ = permeability of free space, $4\pi \times 10^{-7}$ H/m
$\phi$ = $e/kT_e$, V$^{-1}$
$\Omega$ = solid angle of plume expansion, sr
$\Omega^e$ = electron Hall parameter

## Introduction

THE first observations of magnetoplasmadynamic (MPD) thruster operation were reported in 1964.[1] Since then, two main types of MPD thrusters have been investigated, both with performance characteristics of interest for near-Earth and interplanetary missions. The more simple of the two MPD types is the self-field MPD thruster, in which the magnetic field used to accelerate the propellant is generated by thruster current. The applied-field MPD, which evolved later, utilizes external magnets built into the thruster to supply an additional magnetic nozzle with radial and axial field components. The self-induced mode of operation is attractive for space thruster applications because the burden of the external magnet is removed, and significantly more freedom is allowed in the design of the accelerating channel.

Experimental performance for both types of thrusters varies widely, depending on propellant type, thruster type, and power level.[2] Hydrogen and lithium typically give higher efficiencies than those obtained with propellants such as ammonia, argon, or nitrogen. For example, a thrust efficiency of 43% has been obtained with hydrogen in a 1.5-MW pulsed self-field thruster at a specific impulse of 4900 s. Higher values of thrust efficiencies, from 48 to 68%, have been obtained in a steady-state applied-field thruster with lithium at power levels less than 20 kW. With argon propellant, reported efficiencies have not exceeded 35% for specific impulse values in the 2000–

Received May 4, 1992; revision received Oct. 10, 1992; accepted for publication Dec. 11, 1992. 

*Associate Professor, Department of Aeronautical and Astronautical Engineering. Associate Fellow AIAA.
†Graduate Student, Department of Aeronautical and Astronautical Engineering. Member AIAA.
‡Group Leader, Electric Propulsion, Phillips Laboratory, OLAC-PL/RKAS. Member AIAA.

4000 s range, both with pulsed self-field and with low-power applied-field MPD thrusters.[2]

The research described here was undertaken to improve the understanding of the performance limitations of MPD thrusters, through the application of a new quadruple langmuir probe technique. The probe is used with a pulsed argon MPD thruster to measure the physical characteristics of the exhaust plume, including electron temperature, electron density, and flow velocity, and to infer other properties including the heavy particle temperature. With this information it should be possible to develop a better understanding of the propellant acceleration process, leading to improved MPD thruster performance. The technique is also directly applicable to similar plasma flows, e.g., arcjet plumes, which satisfy specified plasma Debye length and mean free path criteria with respect to the probe.

## Description of Experiment

The pulsed MPD thruster (Fig. 1) has a 9-cm-long cylindrical copper anode with an i.d. of 5.08 cm, and a 9-cm-long, 0.95-cm-diam cathode of 2% thoriated tungsten. The tip of the cathode has a full radius of 0.47 cm, and is flush with the anode downstream face ($x = 0$ cm). The anode downstream edge has a 0.32-cm radius. The boron nitride insulating backplate has eight 0.32-cm-diam propellant injection holes symmetrically spaced about the thruster centerline on a 2.54-cm-diam circle. The thruster is mounted on nonconducting supports on a 20-cm steel I-beam in a 2.5-m-diam by 3.8-m-long steel vacuum chamber.[1]

The thruster is driven by a 10-section pulse forming network (PFN) which can provide a 1.1-ms flat top current pulse at a maximum current of 40 kA to the thruster. Each section consists of three 2000-$\mu$F capacitors in parallel and one five-turn 0.53-$\mu$H copper inductor. The PFN impedance is 9.4 m$\Omega$, and

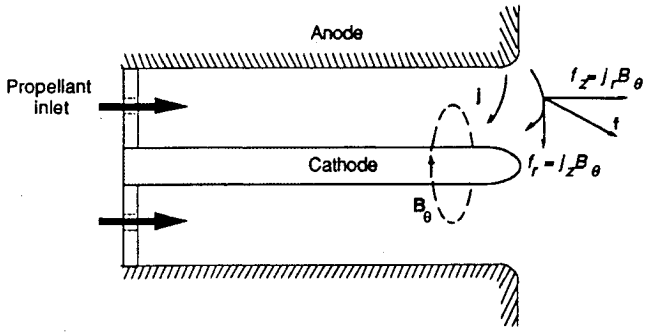


**Fig. 1 Self-field pulsed MPD thruster. Argon propellant is injected through eight holes in the insulating backplate.**

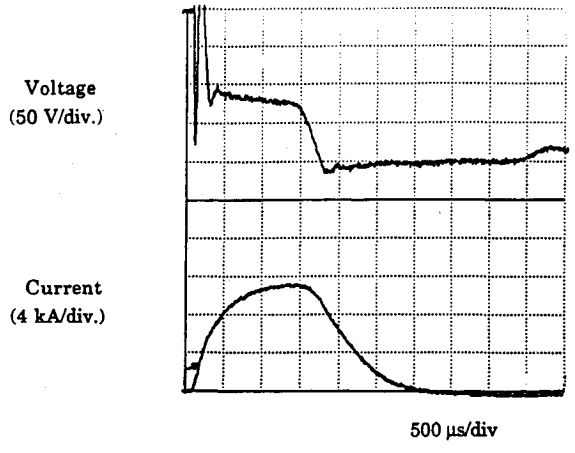


**Fig. 2 Pulsed MPD thruster voltage and current traces. The thruster is operating at 137 V and 11.5 kA.**

the repeatability of the bank voltage is better than 1%. The PFN circuit has no series switch, as full bank voltage appears on the thruster electrodes, and the thruster is fired with a third spark trigger electrode located in the boron nitride backplate.

Argon propellant flow into the thruster is provided by a 3.7-l plenum and solenoid valve located inside the vacuum chamber close to the back of the thruster. Plenum pressure, and hence mass flow rate, is set to $\pm 1\%$ on successive shots. Upon opening the valve, the thruster mass flow rate $\dot{m}$ rises to a steady value in ~10 ms. After ~15 ms of steady flow, the PFN is fired, initiating the 1.1-ms current pulse. Mean tank ambient pressure is $\sim 10^{-3}$ Torr during the current pulse. In this experiment the thruster is operated at a mass flow rate of $\dot{m} = 2 \pm 0.1$ g/s, as determined from the measured pressure drop in the plenum for an 80-ms flow pulse.

Sample thruster voltage (upper trace) and current (lower trace) are shown in Fig. 2. The thruster voltage, after a sharp initial peak, settles to a steady value of $137 \pm 8$ V during the pulse. The current is operated at a steady current level of $11.5 \pm 0.5$ kA for about 500 $\mu$s, and the impedance of the thruster is $11 \pm 0.5$ m$\Omega$, well-matched to the PFN. The thruster is operated at 1.5 MW, below the onset condition,[3-5] which occurs at 15 kA for $\dot{m} = 2$ g/s. After several dozen firings the thruster gradually develops a coating of charred pump oil and must be cleaned.

## Probe Construction

A schematic diagram of the quadruple probe is shown in Fig. 3. Each probe tip is constructed[1] of 0.25-mm-diam tungsten wire mounted in 1.2-mm-diam alumina tubing. The exposed probe length is $5.0 \pm 0.2$ mm, giving a surface area of $A = 4.0 \pm 0.2$ mm$^2$. The tungsten wires are cemented with high-temperature adhesive into the 1.2-mm alumina tubing, which telescopes into four 3.2-mm-diam tubes, cemented into an 18-mm-diam × 1-mm-wall Pyrex® tube containing four RG58 cables, wrapped together with electrically insulating high-temperature tape. The RG58 cables are then connected by means of vacuum feed-throughs to the probe electronics and oscilloscope located near the tank. The probe assembly is mounted on a rigid plastic beam in the vacuum chamber. The probe is located on the thruster axis, and axial positioning is achieved with a motorized X-Y table capable of 0.02-cm accuracy.

The charred coating seen on the thruster is not observed on the probe. Instead, after approximately 60 firings at test conditions, a silvery film of cathode tungsten, with small amounts of iron and gold from the spark trigger electrode, forms on the probe and probe arm. This coating is scraped away at the end of each test period to prevent probe shorting, and is not believed to affect the results.

Probe cleaning was attempted by several minutes of glow discharge ion bombardment at ~600 V,[1] as has been used for a steady thruster.[6] Following cleaning, the probe voltage $V_{d2}$, normally ~2 V, rose to ~8 V for one or two shots, and then returned to the precleaning value. This cleaning approach was therefore rejected in favor of mechanical removal of the silvery coating.

The separation between probe wires (Fig. 3) is approximately 3 mm. Probes 1, 2, and 3 are parallel to the probe

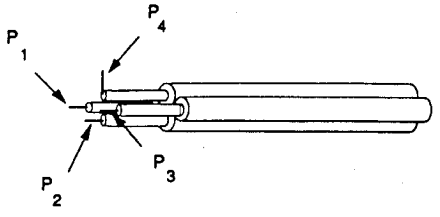


**Fig. 3 Sensing tip of quadruple probe. The probe is aligned so that probes 1–3 are parallel, and probe 4 is perpendicular to the flow.**

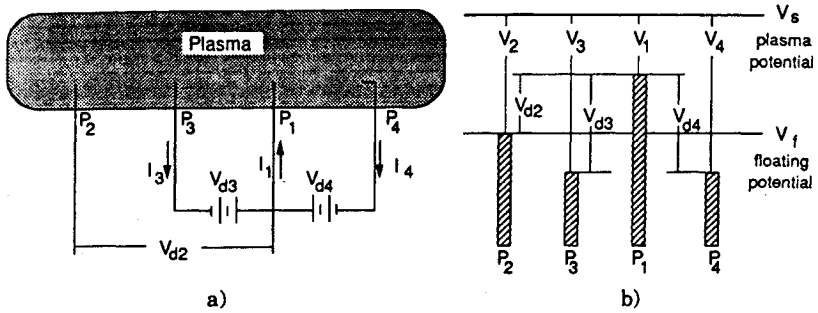


**Fig. 4 Electrical schematic a) and potential plot b) of the quadruple probe. Probe 2 is at the floating potential of the plasma. Probes 3 and 4 are biased by a fixed amount ($V_{d3}$ and $V_{d4}$) relative to probe 1, and the potential difference between probes 1 and 2 ($V_{d2}$) is measured.**

axis, and probe 4 is perpendicular. An electrical schematic and potential plot of the quadruple probe configuration are shown in Fig. 4. Probe 2 is electrically floating ($I_2 = 0$), and the remaining probes collect current $I_1$, $I_3$, and $I_4$.

## Probe Theory

The quadruple probe derives from a combination of triple langmuir probe[6,7] and crossed electrostatic probe techniques,[8-12] and simultaneously measures the electron temperature, electron density, and flow velocity of the plasma. The ion saturation current collected by the perpendicular probe, when compared to the current collected by a flow-aligned probe at the same potential, determines local flow velocity.

Analysis of probe response assumes a maxwellian electron energy distribution. The reasonableness of this assumption depends on a calculation of $\lambda_{ee}$, which is ~2 cm at 8 eV near the cathode, and falls to a few millimeters further out in the plume, small compared to the plume gradient scale length $T_e/dT_e/dx$. The analysis also assumes that the ion sheath surrounding the probe is thin compared to $r_p$. The thickness of the sheath is on the order of the Debye length, [$\lambda_D = 7440(T_e/n_e)^{1/2} = 7440(4/10^{18})^{1/2} = 1.5 \times 10^{-5}$ m], typically a few percent of the probe radius, introducing a few percent increase in effective probe area. Increasingly negative probe potentials tend to increase the sheath thickness, collection area, and ion current, thereby overstating $T_e$ and $n_e$. For argon with $T_e \approx 5$ eV, measured $T_e$ is systematically ~5% too high, and measured $n_e$ approximately 15% too high, due to sheath thickness error. This error is reduced at lower $T_e$.[7]

The probe analysis assumes $\lambda_{ii}/r_p >> 1$. For densities from $10^{18}$–$10^{20}$ m$^{-3}$, and temperatures from 1–10 eV, $10^3 > \lambda_{ii}/r_p > 10$ and the probe sheath is therefore collisionless.

The analysis of quadruple probe response[1] is similar to that for the triple probe.[6,7] All four probes have equal geometric surface area $A$. In supersonic flow with $\lambda_{ii} >> r_p$, the collection area of the perpendicular probe 4 is reduced by a wake region of low ion and electron density, presumed to exist behind the probe.[9,10] In the flow conditions pertaining here, with $u > 3$ times the thermal speed $c_m$ as predicted below by Eq. (4), the ions cannot penetrate the wake region, which has a width ~$2r_p$. The electrons are prevented from doing so by quasi-neutrality despite their high thermal speed, since $\lambda_D/r_p << 1$. Thus, for a stationary plasma the ion collection area is $A = 2\pi r_p L$, whereas for high plasma velocity the ion collection area becomes the projected area; $A_{4,i} = 2r_p L$, while the surface area for electron current to probe 4 is $A_{4,e} = \pi r_p L$.

### Electron Temperature

The probe analysis for a quadruple probe follows that of Chen and Sekiguchi.[7] For $A_1 = A_2 = A_3 = A$, $A_{4,i} = A/\pi$, and $V_{d3} = V_{d4}$, with $j_i$ independent of potential[1]:

$$1 = \frac{1 + \exp(\phi V_{d3}) - 2\exp[\phi(V_{d3} - V_{d2})]}{\{\exp[\phi(V_{d3} - V_{d2})]/\pi - \frac{1}{2}\}} \qquad (1)$$

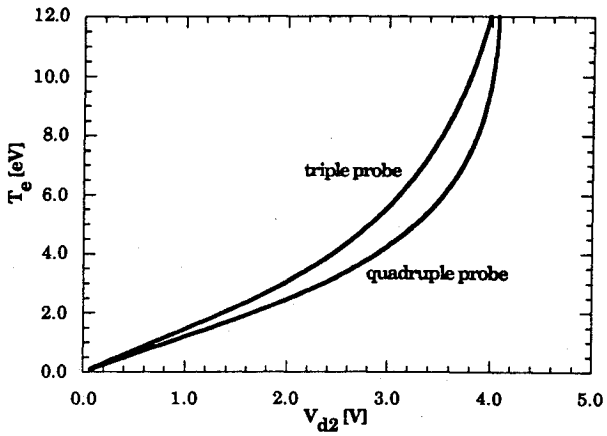


**Fig. 5 Variation of electron temperature $T_e$ with measured potential difference $V_{d2}$ for $V_{d3} = V_{d4} = 10$ V. Quadruple probe (lower) and triple probe (upper).**

Equation (1) permits the determination of $\phi$, and hence, electron temperature from $V_{d2}$ for a fixed value of $V_{d3}$. Figure 5 gives $T_e$ as a function of $V_{d2}$ from Equation (1) for $V_{d3} = V_{d4} = 10$ V.

### Electron Density

The electron density is determined from the ion current density. For an ion-attracting probe, the probe sheath creates an electrostatic field which penetrates the neighboring plasma and attracts ions toward the probe. For a maxwellian energy distribution for the electrons the attractive potential depends both on $T_e$ and the ion energy, and for $T_e \cong T_i$, $j_i$ is approximated in the thin sheath limit by[7]

$$j_i = en_e[k(T_e + T_i)/m_i]^{1/2} \exp(-\tfrac{1}{2}) \qquad (2)$$

Note that this current is larger than that predicted by thermal diffusion. The electron saturation current density is given by[7] $j_{es} = n_e e(kT_e/2\pi m_e)^{1/2}$.

Writing expressions for $j_e$ and $j_i$ at each probe and solving gives an expression for electron density measured by a quadruple probe[1,7]

$$n_e = \frac{3I_3(m_i)^{1/2}\exp(\frac{1}{2})}{2Ae[k(T_e + T_i)]^{1/2}[\exp(\phi V_{d2}) - \pi/4]} \qquad (3a)$$

or

$$n_e = (m_i)^{1/2} f^{IV}(V_{d2}) I_3/A \qquad (3b)$$

The function $f^{IV}(V_{d2})$ is shown in Fig. 6 for $T_e = T_i$. Using this relation $n_e$ can be determined continuously from the simultaneously measured values of $V_{d2}$ and $I_3$.

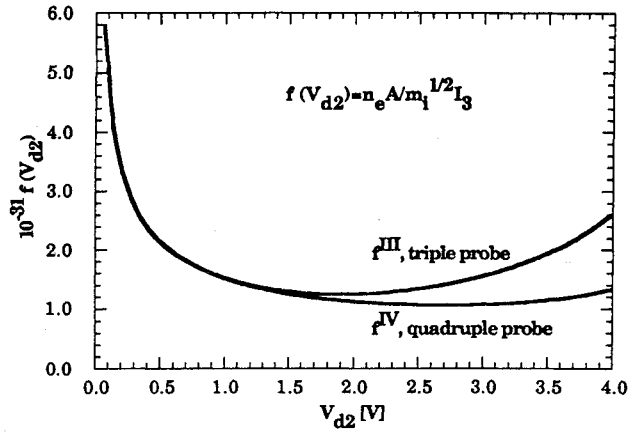


**Fig. 6 Relation between the functions $f^{III}(V_{d2})$ and $f^{IV}(V_{d2})$ and the measured voltage $V_{d2}$ for a fixed voltage of $V_{d3} = V_{d4} = 10$ V. Quadruple probe (lower) and triple probe (upper).**

### Plasma Velocity

For a flow-aligned probe ($\theta = 0$) the ion current is a function of $T_e$ [Eq. (2)]. For a probe at an angle $\theta$ to the flow, the ion current is also a function of $\kappa = (u/c_m)\sin\theta$.[8] The quadruple probe makes use of two probes with areas $A_\parallel$ at $\theta = 0$ deg and $A_\perp$ at $\theta = 90$ deg to measure plasma velocity. For maxwellian ion and electron velocity distributions, the probe current ratio is[8,9]

$$\frac{I_\perp}{I_\parallel} = \frac{2A_\perp}{\sqrt{\pi}A_\parallel} e^{(u/c_m)^2} \sum_{n=0}^{\infty} \left[\frac{(u/c_m)^n}{n!}\right]^2 \Gamma\left(n + \frac{3}{2}\right) \qquad (4)$$

where the wake effect gives $A_\perp/A_\parallel = 1/\pi$. In the present experiment it is determined experimentally that $I_\perp/I_\parallel > 1$, for which Eq. (4) requires that $u/c_m > 3$ and $I_\perp = en_e uA_4/\pi$ to within 3% accuracy.[1,8] Thus, the current $I_\perp$ is directly proportional to $n_e$, to the flow velocity, and to the projected probe area $2r_pL$.

### Operation of Quadruple Probe as a Triple Probe

The quadruple probe can be operated in two modes: four probes connected, which is the preferred mode, or a triple probe mode with either probe 3 or 4 connected, using a triple probe circuit[6,7] similar to that in Fig. 4. By alternating probes 3 and 4 on consecutive shots at repeatable conditions, $T_e$, $n_e$, and $u$ are determined, provided that the potential difference $V_{d3} = V_{d4}$ is not changed.

In the triple-probe mode, Eqs. (1) and (3) for the quadruple probe must be modified to account for the reduced ion saturation current collected with one probe disconnected. The expression determining $T_e$ in the triple-probe mode is

$$\frac{1}{2} = \frac{1 - \exp(-\phi V_{d2})}{1 - \exp(-\phi V_{d3})} \qquad (5)$$

$T_e(V_{d2})$ for the triple probe is shown in Fig. 5.[1,7] The electron density in the triple-probe mode becomes

$$n_e = \frac{I_3(m_i)^{1/2}\exp(\frac{1}{2})}{Ae[k(T_e + T_i)]^{1/2}[\exp(\phi V_{d2}) - 1]} \qquad (6a)$$

or

$$n_e = (m_i)^{1/2} f^{III}(V_{d2}) I_3/A \qquad (6b)$$

The function $f^{III}(V_{d2})$ for the triple-probe mode is shown in Fig. 6 for $T_e = T_i$.

## Experimental Results

All measurements are taken on the centerline of the thruster downstream of the thruster face, at 3.2, 6.3, 12.7, and 25.4 cm. The voltage $V_{d2}$ and current signal $I_3$ from the probe are stored in a dual channel DSA 601 digitizing oscilloscope, and printed out after each shot. The availability of only two channels dictates that the probe be run in the triple-probe mode.

A sample shot for the perpendicular probe (Fig. 7) displays current $I_4$ and voltage $V_{d2}$. The signals shown here are fed through ungrounded 20-kHz low-pass filters to aid data reduction. The high-frequency noise is assumed to have no effect on probe response, which is analyzed in terms of the mean signal amplitude.

Following an initial noise spike, the average probe current and voltage signals are approximately level, predicting little variation in $T_e$, $n_e$, and $u$ during the pulse. At the end of the flat top portion of the pulse, data analysis of the probe signals shows that the flow velocity decays first with a characteristic decay time of 0.2 ms, followed by electron density in 0.4 ms, and electron temperature in 0.9 ms.[1]

## Plasma Flow Properties

The centerline electron temperature 1 ms after the start of the pulse is shown in Fig. 8 as a function of axial probe position for a thruster current of 11.5 ± 0.5 kA and $\dot{m} = 2.0 \pm 0.1$ g/s. Measured $T_e$ is approximately 8 ± 3.5 eV at $x = 3$ cm,

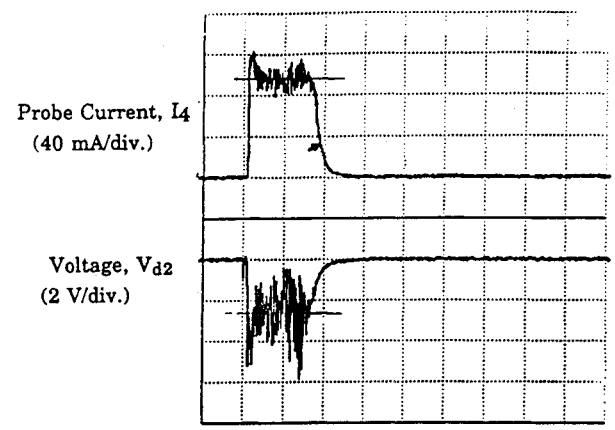


**Fig. 7 Unfiltered current and voltage signals from probe $P_4$, located 6.3-cm downstream, with $I_4 = 96 \pm 8$ mA and $V_{d2} = 2.6 \pm 0.8$ V.**

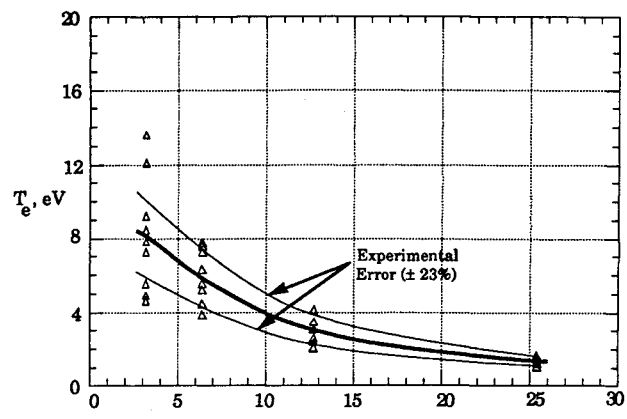


**Fig. 8 Centerline electron temperature at four axial probe positions. The thruster is operated at 137 ± 8 V and 11 ± 0.5 kA at an argon mass flow rate of 2 g/s.**

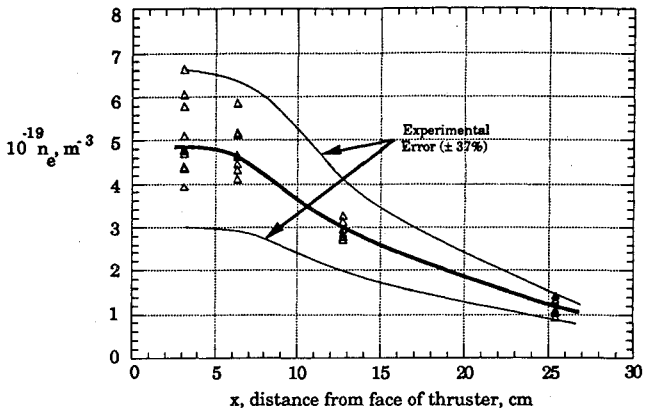


**Fig. 9 Centerline electron density at four axial probe positions. The thruster is operated at 137 ± 8 V and 11 ± 0.5 kA at an argon mass flow rate of 2 g/s.**

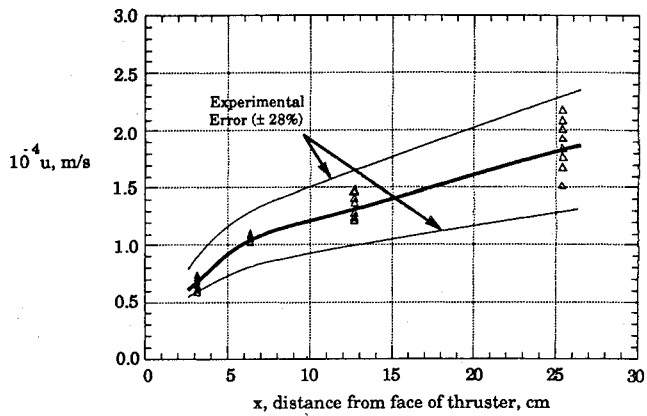


**Fig. 10 Centerline flow velocity at four axial probe positions. The thruster is operated at 137 ± 8 V and 11 ± 0.5 kA at an argon mass flow rate of 2 g/s.**

falling to 1.5 ± 0.3 eV at $x$ = 25.5 cm. In addition to the systematic error in $T_e$ (5%) and $n_e$ (15%) discussed above—caused by finite probe sheath thickness—the estimated experimental random error is ±23%. Contributions to the error come from noise on the voltage signal (±20%), nonzero $\alpha^{++}$ and probe surface area (±10%),[6] and the assumption of constant ion saturation current (±5%).[7] The error caused by probe misalignment (<2 deg) has been measured for collisionless plasma conditions and found to be less than 2% for a misalignment of 3 deg.[10] The spread in $T_e$ (Fig. 8) close to the thruster face may be caused by asymmetries in the plasma discharge. Pitting of the anode is observed at a few azimuthal locations, as would be caused by filamentary spoking of the radial current, a common occurrence in MPD thrusters.

The centerline electron density is shown in Fig. 9. The spread in $n_e$ is largest close to the thruster, and falls within experimental error at distances beyond 5 cm from the thruster face. The estimated error is ±37%, with the largest contributions from probe end effects and doubly charged ions (±30%),[6] the increase in sheath thickness (±14%) and signal noise (±22%).

Centerline flow velocity $u$ is shown in Fig. 10. Velocity increases throughout the plume from 0.7 ± 0.15 × $10^4$ m/s at $x$ = 3 cm to 1.8 ± 0.5 × $10^4$ m/s at $x$ = 25 cm. The estimated error is ±28%, with the largest sources from the variation in sheath thickness (±14%) and from signal noise (±24%).

## Discussion

The measured centerline electron temperature, electron density, and flow velocity of the plasma are in general accord with the results obtained in other experiments on quasisteady MPD thrusters, as shown in Table 1. Bruckner and Jahn[17] spectroscopically determined an ion velocity of $10^4$ m/s at $x$ = 6 cm and 1.7 × $10^4$ m/s at $x$ = 42 cm, for a 16 kA, 6 g/s argon MPD thruster. Tahara et al.[18] using a double langmuir probe, observed an electron temperature along the centerline of the thruster of 6 eV at 2-cm downstream from the cathode tip, falling to 1 eV at 18 cm. These $T_e$ values are similar to those obtained in the present experiment. The electron density along the centerline of the thruster[18] was 2 × $10^{21}$ $m^{-3}$ at 2-cm downstream of the thruster, and 1 × $10^{20}$ $m^{-3}$ at 18 cm. Spectroscopic velocity measurements made in the same experiment gave an axial velocity along the centerline of 1 × $10^4$ m/s close to the thruster and 2 × $10^4$ m/s further out in the plume. Jahn et al.[19] used two sets of double langmuir probes, one a set distance downstream of the other, to measure velocity at locations from 2.5- to 30-cm downstream of a quasisteady MPD thruster, operating at 17 kA with argon propellant. Velocity was measured at 2 × $10^4$ m/s leaving the anode to approximately 3 × $10^4$ m/s, 30-cm downstream. Electron temperature and density were also measured at one location using a single langmuir probe. At 30-cm downstream of the thruster, $T_e$ was 1.4 eV and $n_e$ was 1.2 × $10^{19}$ $m^{-3}$.

The measured properties $T_e$, $n_e$, and $u$ can be used to evaluate plasma flow properties. Calculation of $\lambda_{ee}$ gives a variation from 20 mm at the face of the thruster to 1-mm downstream, so that the plasma can be approximated as a continuum with a locally maxwellian velocity distribution. Calculation of the Debye length gives $\lambda_D/r_p \leq 0.05$, sufficiently small to validate the thin-sheath assumption. Calculation of ion-ion mean free path validates the collisionless-sheath assumption since $\lambda_{ii}/r_p \geq 10^2$, assuming single ionization. The ion-neutral mean free path is ~1 cm near the thruster and ~5 cm far downstream.

A clue to the expansion process in the plume is provided by plotting $T_e$ vs $n_e$ at several positions (Fig. 11). For an adiabatic electron plume expansion, roughly valid here because the downstream current density is small and elastic and inelastic electron-heavy particle energy transfer collisions are infrequent, the electron temperature varies as $T_e \sim n_e^{\gamma-1}$. Plotted in Fig. 11 are slopes corresponding to several values of $\gamma$, which indicate that the effective $\gamma$ lies between 2 and 3. This value is consistent with an expansion in which the electrons gyrate around the $B_\theta$ lines with $\Omega^e >> 1$,[20] which holds for $T_e > 3$ eV and $B_\theta > 10^{-2}$ T. Magnetic fields of this magnitude have been measured at $x$ = 6 cm and a radius of 2 cm off the centerline, but not on the centerline. The apparent involvement shown here of the $B_\theta$ field in the expansion process requires further investigation.

At lower $T_e$ further downstream $\Omega^e < 1$, so that the electrons decouple from $B_\theta$ and $\gamma = \frac{5}{3}$ is appropriate. For the hot ions the Larmor radius is larger than the anode radius, the ion-neutral mean free path is several cm, and the effective $\gamma$ for ions is therefore also $\frac{5}{3}$.

Calculation of the mean free path for both electron-neutral impact ionization collisions and three-body recombination collisions shows that both of these events are infrequent, so that the ionization process is frozen a few centimeters downstream. If it is assumed that the plume plasma expands spherically as a uniform jet of solid angle $\Omega$ from a virtual center

**Table 1 Comparison of MPD centerline plume measurements in argon**

| | Anode ID, cm | $I$, kA | Max $u$, m/s | Downstream $T_e$, eV | Downstream $n_e$, $m^{-3}$ |
|---|---|---|---|---|---|
| Present experiment | 5 | 11.5 | 18,000 | 1.2 | 1.2 × $10^{19}$ |
| Bruckner et al.[17] | 10 | 16 | 17,000 | 0.8 | — |
| Tahara et al.[18] | 5 | 10 | 18,000 | 1.0 | 10 × $10^{19}$ |
| Jahn et al.[19] | 10 | 17 | 27,000 | 1.4 | 1.2 × $10^{19}$ |

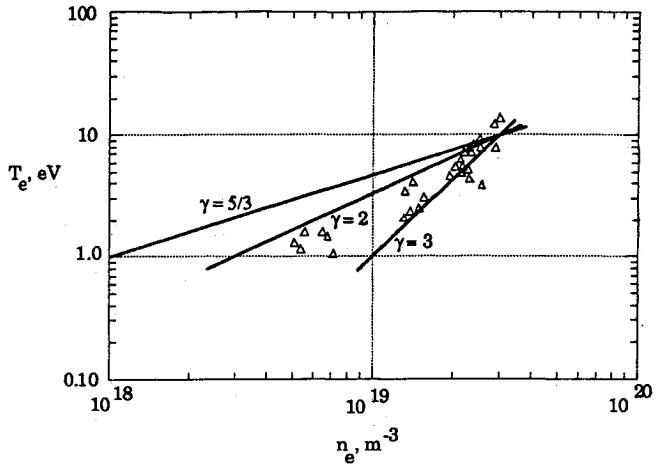


**Fig. 11 Centerline electron temperature vs electron density. The data follow an isentropic expansion with $2 < \gamma < 3$.**

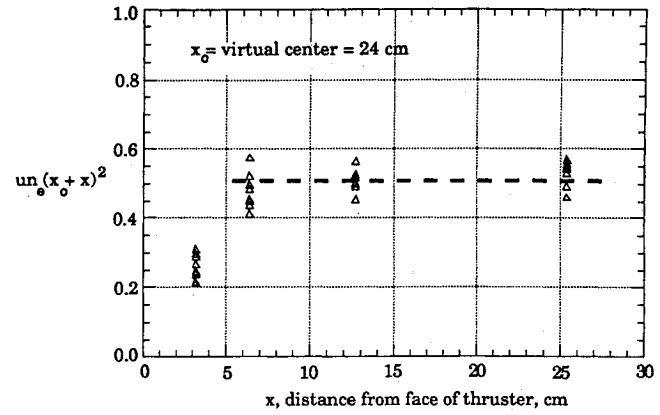


**Fig. 12 Calculated charged particle flow rate $un_e(x_0 + x)^2$, assuming a spherical expansion with virtual center $x_0$ located 24 cm behind the face of the thruster.**

at $x_0$, and if $n_e$ and $u$ are assumed to depend only on expansion distance, then the charged particle flow rate $un_e(x_0 + x)^2\Omega$ will be constant for the proper choice of $x_0$. Figure 12 shows that for centerline values of electron density and velocity, the quantity $un_e(x_0 + x)^2$ becomes constant at large $x$ for $x_0 =$ 24 cm. For $x < 5$ cm, the flow does not expand spherically, presumably because the plasma is undergoing $\mathbf{j} \times \mathbf{B}$ acceleration in this region. The solid angle determined by the anode radius and $x_0 = 24$ cm is $\Omega = 0.034$ sr (half-angle = 6 deg).

The ion-neutral mean free path at $x = 6$ cm is a few mm, so that the heavy particles are collisionally coupled. A lower limit on the average neutral density near the thruster can be estimated from $\dot{m} \approx 2\pi unx^2$, assuming spherical expansion of the neutrals from the cathode tip into a $2\pi$ solid angle at the local ion velocity $u = 1.0 \times 10^4$ m/s. At $\dot{m} = 2$ g/s the estimated density is then $n = 1.3 \times 10^{20}$ at $x = 6$ cm, corresponding to $\alpha = 0.26$.

The above low $\alpha$ estimates imply that $\alpha^{++}$ may be small, despite the high temperatures near the cathode where $T_e \approx$ 8 eV. For an equilibrium 0.1 atm argon plasma at 1 eV, $\alpha =$ 0.27 and $\alpha^{++} = 2.0 \times 10^{-7}$.[21] This low $\alpha^{++}$ result is favorable for interpretation of probe results, since $\alpha^{++}$ reduces $n_e$ for a given probe current by a factor of $2\sqrt{2T_e}$. Although spectroscopic studies of MPD plumes have noted the presence of doubly ionized argon,[16,17] no estimates are known of ionization fraction for these particles.

The probe results for velocity suggest that high values of ion temperature exist in the thruster plume. From separate B-probe measurements on this thruster, the enclosed thruster current is less than 1% of the total current for $r < 2$ cm and $z > 5$ cm. Assuming that for $x > 5$ cm $\mathbf{j} \times \mathbf{B} \approx 0$, ionization and excitation are frozen, and the heavy particles are in translational equilibrium, the increase in $u$ from $1.0 \times 10^4$ at $x =$ 6 cm to $1.8 \times 10^4$ at $x = 25$ cm implies an argon temperature drop in that distance of $\Delta T = \Delta(u^2/2C_p) \approx 18$ eV. For an isentropic heavy particle expansion at $\gamma = \frac{5}{3}$, the observed density drop in the plume of a factor of 4 implies that the temperature varies as $\sim n^{\gamma-1} = 2.5$, giving $T \sim 12$ eV at $x =$ 25 cm and $T \sim 30$ eV at $x = 6$ cm for $\Delta T = 18$ eV. At 30 eV the sound speed is $\sim 1.1 \times 10^4$, indicating sonic conditions near $x = 6$ cm, and implying subsonic flow inside the thruster. The total temperature is $T_0 \approx [(\gamma + 1)/2](30) \sim 40$ eV, significantly higher than $T_e$, and the ion Mach number is $M \approx 2.5$ at $x = 25$ cm. Despite this high ion temperature the pressure near the cathode is $nkT_0 \sim 600$ Pa, a level generated by <1 kA pumping the plasma radially at the cathode tip.

For ion temperature higher than $T_e$ the probe response to electron temperature is not affected, but a correction must be made to the experimentally measured electron density. The effect of high ion energy is rigorously presented by Lam[23] fo a maxwellian collisionless plasma with $\lambda_D/r_p \ll 1$, and predicts a saturation current density different from that in Eq. (2)[7]:

$$(j_i)_{\text{Lam}} \cong (en_e/\pi)[2k(T_e + 4T_i/\pi)/m_i]^{1/2} \qquad (7)$$

For $T_i = T_e$, using Lam's Eq. (7) instead of Eq. (2) to calculate $n_e$ gives a density which is higher than that in Eq. (6) by a factor $\pi e^{-1/2}(1 + 4/\pi)^{-1/2} = 1.26$. For $T_i = 30$ eV and $T_e$ = 8 eV, the predicted density from Lam drops by a factor $\pi e^{-1/2}[1 + (4/\pi)(30/8)]^{-1/2} = 0.79$. Therefore, with $T_i/T_e \sim$ 4 in the plume, the densities shown in Fig. 9 are too high by about 25%.

The suggested high values of $T$ are consistent with an ion-conduction model of the MPD thruster proposed by Stratton.[22] If the ions fall without collision toward the cathode through a potential drop $\Delta V$, then the total temperature is related to $\Delta V$ by $\Delta V = (\frac{5}{2})kT_0/e$. For $T_0 \approx 40$ eV, $\Delta V \approx 100$ V, consistent with the 140 V observed at the electrodes when allowance is made for sheath drops.

## Conclusions

A quadruple probe has been used for centerline measurements of $n_e$, $T_e$, and $u$ in the plume of a pulsed 1.5-MW argon MPD thruster. Plasma conditions in the plume are found to be appropriate for the application of existing langmuir probe theory.

Analysis of the probe data reveals that the plume expansion process is highly nonequilibrium. The data indicate that ion velocity in the plume increases from 10 to 18 km/s, and that an adiabatic expansion of the charged particles occurs at a small solid angle in the near plume at $2 < \gamma < 3$. This expansion corresponds to ion and neutral temperatures near the cathode of 30–40 eV, significantly higher than the measured $T_e$ of 8 eV near the cathode. While the $T_e$ measured here is higher than the 1–2 eV often seen in extended MPD thruster plumes, it is in near-agreement with other centerline measurements, suggesting that the volume of high $T_e$ plasma is small and close to the cathode tip.

Despite high plume temperatures, electron density measurements indicate that the plume is partially ionized, and therefore, heavily populated with neutrals. Although the charged particles appear to expand with a small solid angle, the neutrals would not be so constrained. The probable existence of high neutral temperatures in the near plume and the absence of a physical nozzle suggests a roughly hemispherical expansion of neutrals. Since the thrust produced by a high-solid angle flow of neutrals is only about half that of

an equivalent flow of charged particles in a narrow beam, partial ionization would significantly reduce thrust efficiency.

## Acknowledgments

We gratefully acknowledge the enthusiastic interest and assistance of S. Castillo, A. Sutton, G. Stiles, D. Tilley, and W. Schmidt of the Phillips Laboratory, Edwards Air Force Base, California.

## References

[1]DelMedico, S. G., "Plasma Flow Measurements by a Quadruple Probe in a Quasi-Steady MPD Plasma," M.S. Thesis, Dept. of Aeronautical and Astronautical Engineering, Univ. of Illinois, Urbana, IL, 1992.

[2]Sovey, J. S., and Mantenieks, M. A., "Performance and Lifetime Assessment of MPD Arc Thruster Technology," AIAA Paper 88-3211, July 1972.

[3]Malliaris, A. C., John, R. R., Garrison, R. L., and Libby, D. R., "Quasi-Steady MPD Propulsion at High Power," NASA CR-111872, 1972.

[4]King, D. Q., Clark, K. E., and Jahn, R. G., "Effect of Choked Flow on Terminal Characteristics of MPD Thrusters," AIAA Paper 81-0686, April 1981.

[5]Subramaniam, V. V., and Lawless, J. L., "Onset in Magnetoplasmadynamic Thrusters with Finite-Rate Ionization," *Journal of Propulsion and Power*, Vol. 4, No. 6, 1988, pp. 526–532.

[6]Tilley, D. L., Kelly, A. J., and Jahn, R. G., "The Application of the Triple Probe Method to MPD Thruster Plumes," AIAA Paper 90-2667, July 1990.

[7]Chen, S. L., and Sekiguchi, T., "Instantaneous Direct-Display System of Plasma Parameters by Means of Triple Probe," *Journal of Applied Physics*, Vol. 36, No. 8, 1965, pp. 2363–2375.

[8]Kanal, M., "Theory of Current Collection of Moving Cylindrical Probes," *Journal of Applied Physics*, Vol. 35, June 1964, pp. 1697–1703.

[9]Johnson, B. H., and Murphree, D. L., "Plasma Velocity Determination by Electrostatic Probes," *AIAA Journal*, Vol. 7, Oct. 1969, pp. 2028–2030.

[10]Poissant, G., and Dudeck, M., "Velocity Profiles in a Rarefied Argon Plasma Stream by Crossed Electrostatic Probes," *Journal of Applied Physics*, Vol. 58, Sept. 1985, pp. 1772–1779.

[11]Maisenhälder, F., and Mayerhofer, W., "Jet-Diagnostics of a Self-Field Accelerator with Langmuir Probes," *AIAA Journal*, Vol. 12, Sept. 1974, pp. 1203–1209.

[12]Chen, S. L., "Studies of the Effect of Ion Current on Instantaneous Triple-Probe Measurements," *Journal of Applied Physics*, Vol. 42, Jan. 1971, pp. 406–412.

[13]Allen, J. E., Boyd, R. L. F., and Reynolds, P., "The Collection of Positive Ions by a Probe Immersed in a Plasma," *Proceedings of the Physical Society B*, Vol. 70, March 1971, pp. 297–304.

[14]Jakubowski, A. K., "Effect of Angle of Incidence on the Response of Cylindrical Electrostatic Probes at Supersonic Speeds," *AIAA Journal*, Vol. 10, Aug. 1972, pp. 988–995.

[15]Bruce, C., and Talbot, L., "Cylindrical Electrostatic Probes at Angles of Incidence," *AIAA Journal*, Vol. 13, Sept. 1975, pp. 1236–1238.

[16]Myers, R. M., "Plume Characteristics of MPD Thrusters: A Preliminary Examination," AIAA Paper 89-2832, July 1989.

[17]Bruckner, A. P., and Jahn, R. G., "Exhaust Plume Structure in a Quasi-Steady MPD Accelerator," *AIAA Journal*, Vol. 12, Sept. 1974, pp. 1198–1203.

[18]Tahara, H., Yasui, H., Kagaya, Y., and Yoshikawa, T., "Experimental and Theoretical Researches on Arc Structure in a Self-Field Thruster," AIAA Paper 87-1093, May 1987.

[19]Jahn, R. G., Clark, K. E., Oberth, R. C., and Turchi, P. J., "Acceleration Patterns in Quasi-Steady MPD Arcs," AIAA Paper 70-165, Jan. 1970.

[20]Sutton, G. W., and Sherman, A., *Engineering Magnetohydrodynamics*, McGraw-Hill, New York, 1965.

[21]Drellishak, K. S., Knopp, C. F., and Cambel, A. B., "Partition Functions and Thermodynamic Properties of Argon Plasma," Gas Dynamics Lab., Northwestern Univ., Arnold Engineering Development Center TDR-63-146, Evanston, IL, Aug. 1963.

[22]Stratton, T. F., "High Current Steady State Coaxial Plasma Accelerators," *AIAA Journal*, Vol. 3, Oct. 1965, pp. 1961–1963.

[23]Lam, S. H., "Unified Theory for the Langmuir Probe in a Collisionless Plasma," *Physics of Fluids*, Vol. 8, Jan. 1965, pp. 73–87.